

# EXPERIMENTAL OBSERVATIONS ON MATERIAL DAMPING AT CRYOGENIC TEMPERATURES

Chia-Yen Peng<sup>1a</sup>, Marie Levine<sup>a</sup>, Lillian Shido<sup>a</sup>, Robert Leland<sup>a</sup>

<sup>a</sup>Jet Propulsion Laboratory, 4800 Oak Grove Drive, Pasadena, CA, USA, 91109-8099

## ABSTRACT

This paper describes a unique experimental facility designed to measure damping of materials at cryogenic temperatures for the Terrestrial Planet Finder (TPF) mission at the Jet Propulsion Laboratory. The test facility removes other sources of damping in the measurement by avoiding frictional interfaces, decoupling the test specimen from the support system, and by using a non-contacting measurement device. Damping data reported herein are obtained for materials (Aluminum, Aluminum/Terbium/Dysprosium, Titanium, Composites) vibrating in free-free bending modes with low strain levels ( $< 10^{-6}$  ppm). The fundamental frequencies of material samples are ranged from 14 to 202 Hz. To provide the most beneficial data relevant to TPF-like precision optical space missions, the damping data are collected from room temperatures (around 293 K) to cryogenic temperatures (below 40 K) at unevenly-spaced intervals. More data points are collected over any region of interest. The test data shows a significant decrease in viscous damping at cryogenic temperatures. The cryogenic damping can be as low as  $10^{-4}$  %, but the amount of the damping decrease is a function of frequency and material. However, Titanium 15-3-3-3 shows a remarkable increase in damping at cryogenic temperatures. It demonstrates over one order of magnitude increase in damping in comparison to Aluminum 6061-T6. Given its other properties (e.g., good stiffness and low conductivity) this may prove itself to be a good candidate for the application on TPF. At room temperatures, the test data are correlated well with the damping predicted by the Zener theory. However, large discrepancies at cryogenic temperatures between the Zener theory and the test data are observed.

## 1. INTRODUCTION

The Terrestrial Planet Finder (TPF) mission is a key element of NASA's Office of Space Science (OSS) Navigator Program and is part of the roadmap for the OSS Astronomical Search for Origins (ASO) science theme. TPF's science objective is to implement NASA's new Vision: "conduct telescope searches for Earth-like planets and habitable environments around other stars" [1]. Specifically, the defining science goal for TPF is to detect radiation from Earth-like planets located in the habitable zones of solar-type stars in order to understand the formation and evolution of planets and, ultimately, of life beyond our Solar System. There are many significant technological challenges existing for all candidate TPF architectures currently studied. A detailed description of the mission and the multiple prong approach for achieving the aggressive goals has been presented at several SPIE conferences recently [2, 3].

One of the challenges is to determine the damping used in characterizing and modeling the cryogenic dynamic behavior of TPF structure and mechanical elements in order to enable accurate system level models for prediction and control of instrument disturbances. Hence the first goal of the present cryogenic damping experiments is to bound the damping values for use in cryogenic structures. This will start with the investigation of material damping and damping mitigation strategies. Note that the most basic vibration damping of any built-up structure derives from the contribution of structural material itself as opposed to the usual structural damping from structural joints. However, material damping is a function not only of material, but also of the following factors:

- Temperature
- Frequency
- Geometry
- Configuration
- Strain sense and amplitude
- Environmental effects

---

<sup>1</sup> [Chia-Yen.P.Peng@jpl.nasa.gov](mailto:Chia-Yen.P.Peng@jpl.nasa.gov); phone 818-354-1285

In the case of laminated composite materials, fiber volume ratio, lay-up orientation, and internal damage from past loading events also play a significant role. This complicates the comparison between different tests and makes it difficult to extrapolate test results to other situations that are under the conditions different from the test.

Levine and White have conducted a good review of the material damping measurements that have been reported in the literature [4].

In order to reduce the thermal emissions of telescope's mirrors and their supporting structures, the TPF telescope system will be operated at cryogenic temperatures, around 40 K. This is essential to achieving the required signal-to-noise ratios for the observations. Very low levels of structural vibration are also required. Associated with small strains and extremely cold temperatures is the expected diminution of structural damping. Low structural damping degrades the quality of the optical alignment by increasing the amplitude of vibration response to on-board dynamic disturbances and by increasing the settling jitter time after spacecraft slews and maneuvers. Therefore, TPF's ability to meet its ambitious science goals will be significantly enhanced by increasing its structural damping at cryogenic temperatures. Given the low inherent structural damping at cryogenic temperatures, significant reduction in vibration amplitude could be gained with only modest increases in damping on the structure.

To resolve the above-described cryogenic damping issues for TPF, the main objectives of the on-going experimental effort described in this paper are:

- Providing an insight into the material damping levels at cryogenic temperatures to enable accurate system level models for prediction and control of instrument disturbances;
- Searching for materials with high cryogenic damping to improve the dynamic stability of cryogenic structures.

The following sections describe the experimental setup, theoretical background of the Zener damping model, data analysis, and our experimental observations on the material damping of Aluminum, Aluminum/Terbium/Dysprosium, Titanium and Composites. In general, the testing described herein to characterize material damping at cryogenic temperatures is unique and has not been reported or performed previously - to the best of authors' knowledge.

## 2. TEST CONFIGURATION & SETUP

As illustrated in Figure 1, the Cryocooler Characterization Lab at the Jet Propulsion Laboratory provided a good test facility for all material damping measurements reported in this paper. The tests were performed inside a 0.6 m diameter thermal vacuum chamber equipped with a Gifford-McMahon cycle cryocooler. The system is capable of maintaining the cold finger at any arbitrary temperature between 293 K and 11 K, but for various practical reasons the minimum specimen temperature achieved was 17 K. During the heating or cooling process, the specimen temperature was closely monitored through the Lakeshore 340 Temperature Controller, Figure 2, which was run on a Labview program. Pressure inside the chamber was maintained between  $10^{-5}$  to  $10^{-6}$  Pa.

Typical cryogenic damping test specimens, Figures 3a and 3b, were prismatic rectangular beams with length 508 mm (20 inch), height 50.8 mm (2 inch), and thickness that varied among specimens. An aluminum frame fixture, Figures 1 and 4, within the chamber supported the specimen as a pendulum and served as a mounting platform for accessories such as mechanical linkages which control the height of the specimen. Two stainless steel suspension wires of 0.281 mm diameter and 838 mm length were used to suspend the specimen from the aluminum frame fixture. In order to minimize interaction between the specimen bending mode and the modes of the suspension system, the two suspension wires were attached to the top edge of the specimen at the two nodal points of the first transverse free-free bending mode.

The specimen was struck quickly by an impact force. In the initial configuration, a 20 mm diameter solenoid actuator controlled by a switch was used to quickly strike the specimen. For the present tests, a refined technique was employed to enable a repeatable impact force to strike the specimen [4]. This technique replaces the solenoid striker with a curved tube, Figure 1, which guides a 6 mm diameter plastic ball through free-fall to collide with the specimen horizontally. The magnitude of impact force is determined by the mass of the ball.

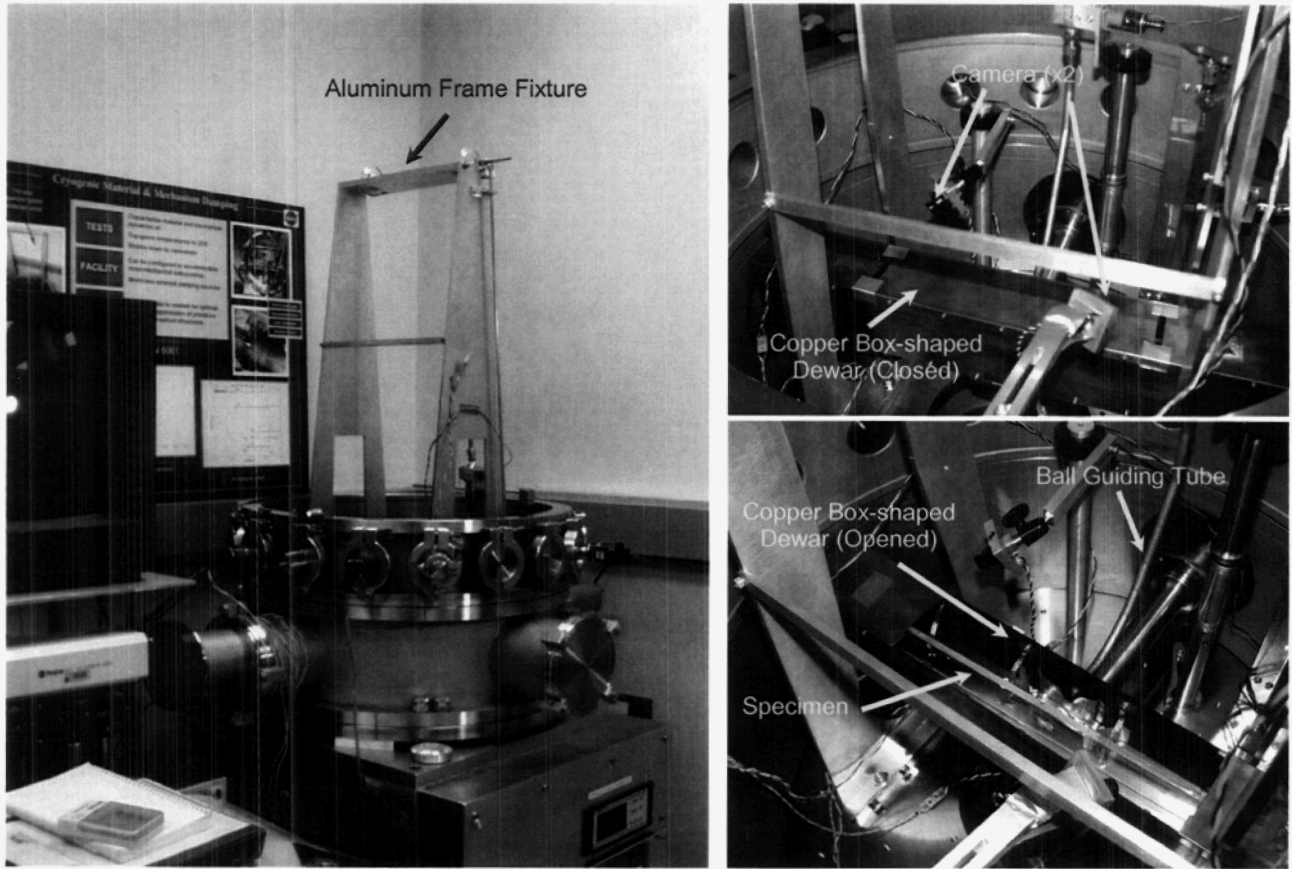


Figure 1. Overview of Cryogenic Damping Test Setup at JPL Cryocooler Characterization Lab

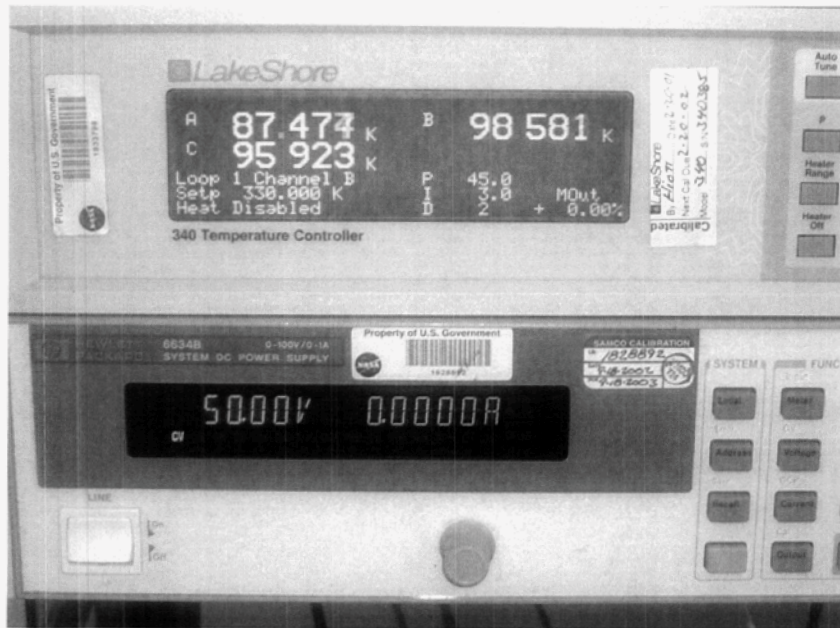


Figure 2. LakeShore 340 Temperature Controller

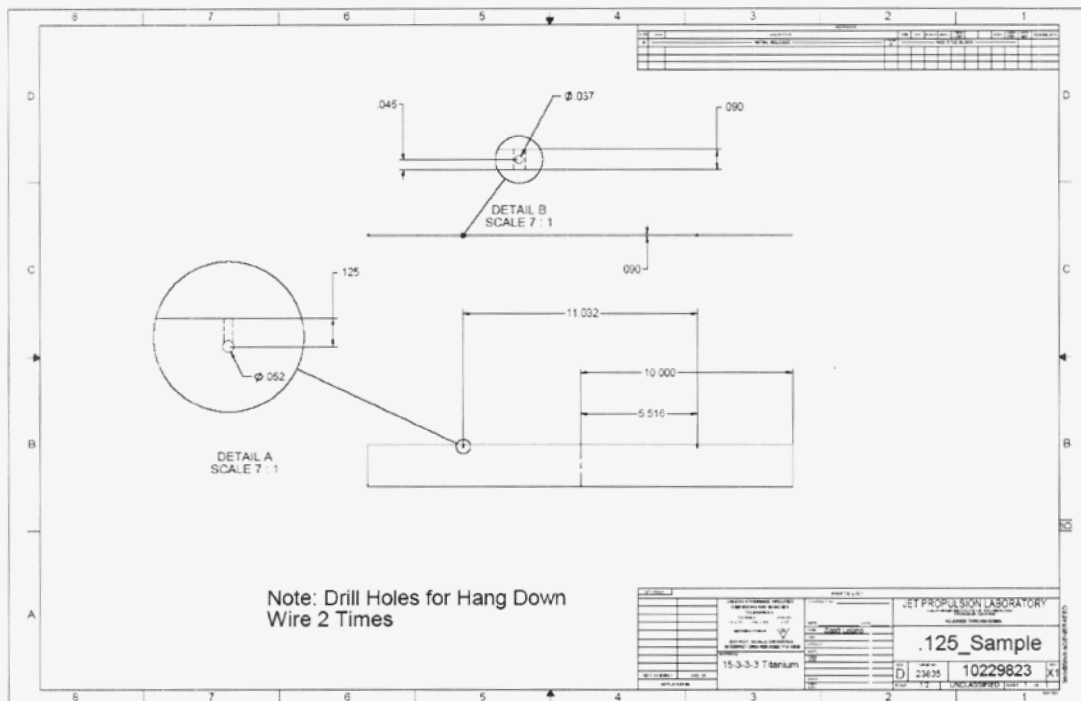


Figure 3a. Key Dimensions of Cryogenic Damping Test Specimen

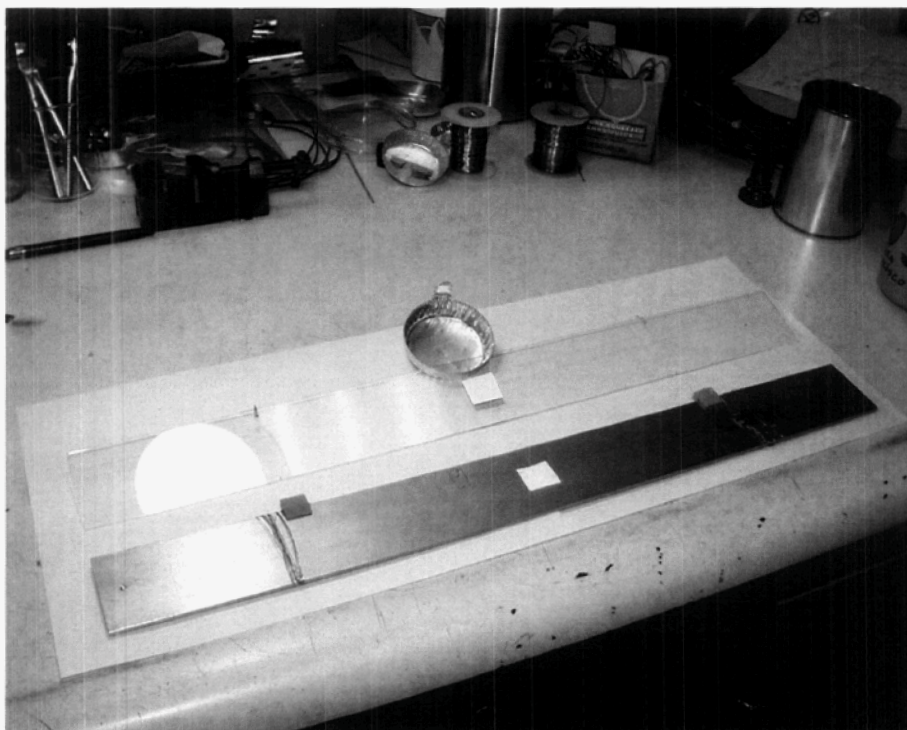


Figure 3b. Close-up of specimens Showing Support Points and Retro-reflective Tape

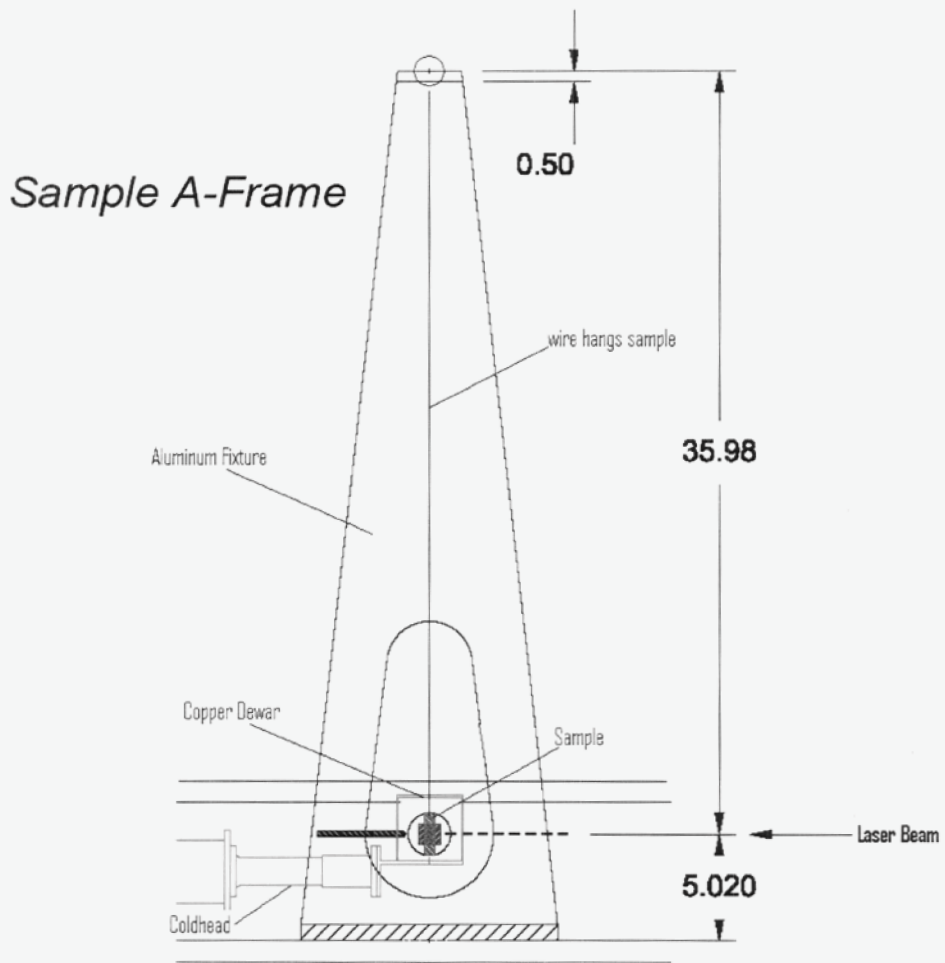


Figure 4. Side View of Aluminum Frame Fixture Setup with Dewar and Coldhead

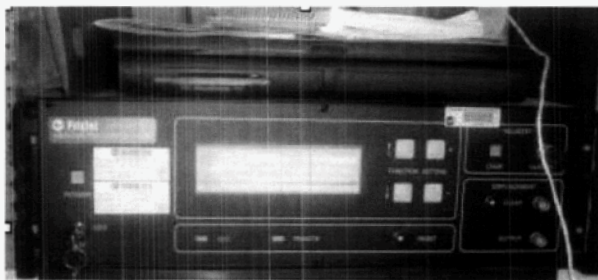


Figure 5. Polytec OFV 3001 Laser Vibrometer

To shield the specimen from radiation heating, the specimen was enclosed in a copper box-shaped dewar, Figure 1, wrapped in a multi layer insulation blanket. The dewar had small openings for the two specimen suspension wires, for the laser beam to measure the specimen response, and for the curved tube. A temperature sensor (8 mm diameter, 1 gram, brass temperature diode) was epoxied to the specimen just underneath one of the suspension wires. The 0.30 mm sensor lead wire was carefully run up the suspension wire with sufficient slack in the lead to minimize interaction. Additional temperature sensors were used to monitor critical locations within the chamber.

The apparent damping estimates could be increased by at least factor of 2 when a high sensitivity piezoelectric strain gauge and a cryogenic accelerometer were used as witness sensors of the vibrating specimen. The additional damping was induced by the small wires connecting to the sensors [4]. Therefore, these sensors were replaced with a non-contacting laser device, Polytec OFV 3001 Vibrometer, Figure 5, to measure transverse velocities of the vibrating specimen. To enhance the optical diffusivity of the specimens, a 25 mm square piece of retro-reflective tape, Figure 3b, was attached as a target for the laser beam. Both the impact force and the laser measurements occurred at the geometrical center of the specimen.

Note that a helium tank was attached to the vacuum chamber in later tests in order to control the temperature of the specimen more effectively. The helium was used as a thermal conductor and played a key role in reaching the minimum temperature of 17 K for the composites - the previous limits were around 40 K. To control the temperature of the specimen, the helium gas was released inside the chamber to a pressure level of  $10^{-4}$  to  $10^{-5}$  Pa and then evacuated as the specimen approached the desired temperature.

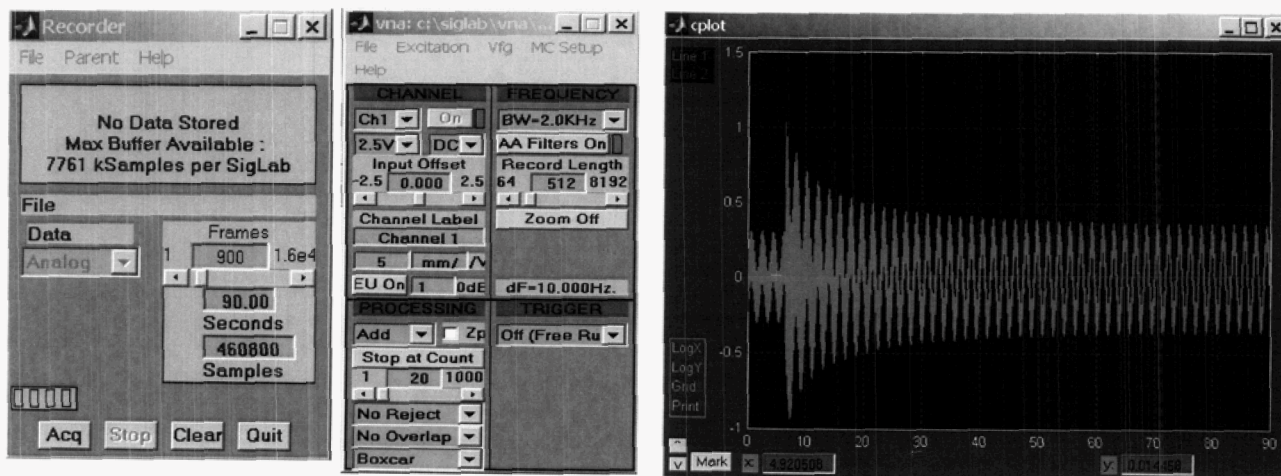


Figure 6. SigLab Data Acquisition System

### 3. DATA ACQUISITION & ANALYSIS

The SigLab Data Acquisition System, Figure 6, was used to acquire data. This system allows simultaneous monitoring and recording of the data. Acquisition of data started 5 seconds before the specimen was to be excited and continued for 60 seconds total or 55 seconds after the specimen was excited. Absolute velocity of the swinging and vibrating specimen was measured with the laser vibrometer and sampled and digitized with a 16 bit data acquisition system. Depending on the specimen and the expected damping, record lengths of up to 60 seconds at a rate of between 5120 samples/sec and 10240 samples/sec were recorded.

As the specimen was excited by striking with an impact force, the specimen vibration decay, Figure 7, was measured by the non-contacting laser vibrometer was used to determine viscous damping ratios. A digital band-pass filter was applied in the forward and backward directions around the fundamental bending frequency to remove all other modes of vibration and the swinging and twisting pendulum motions.

Measured velocities were then converted to extreme fiber strains using the analytical solution for the fundamental mode shape of a free-free beam, in conjunction with the strain-displacement relationship for Euler-Bernoulli beam theory. The result is dependent only on frequency of vibration and beam thickness (both of which are measured directly), not on material properties. After filtering, the record was searched sequentially and the sample with the maximal positive value in each cycle of vibration was selected and retained, to form an envelope of decaying peak amplitudes.

Working with 250 peak values at a time, a least-squares regression analysis was used to compute the best viscous damping coefficient for that window of data. The 250-sample window was then advanced one peak forward in time and the regression analysis was repeated, continuing until the entire record length had been analyzed and an estimate of viscous damping versus time (or peak amplitude) had been formed. For most records, it was then necessary to average this result across the entire time record because of leakage in the damping estimate at the swinging frequency of the specimen in the pendulum mode.

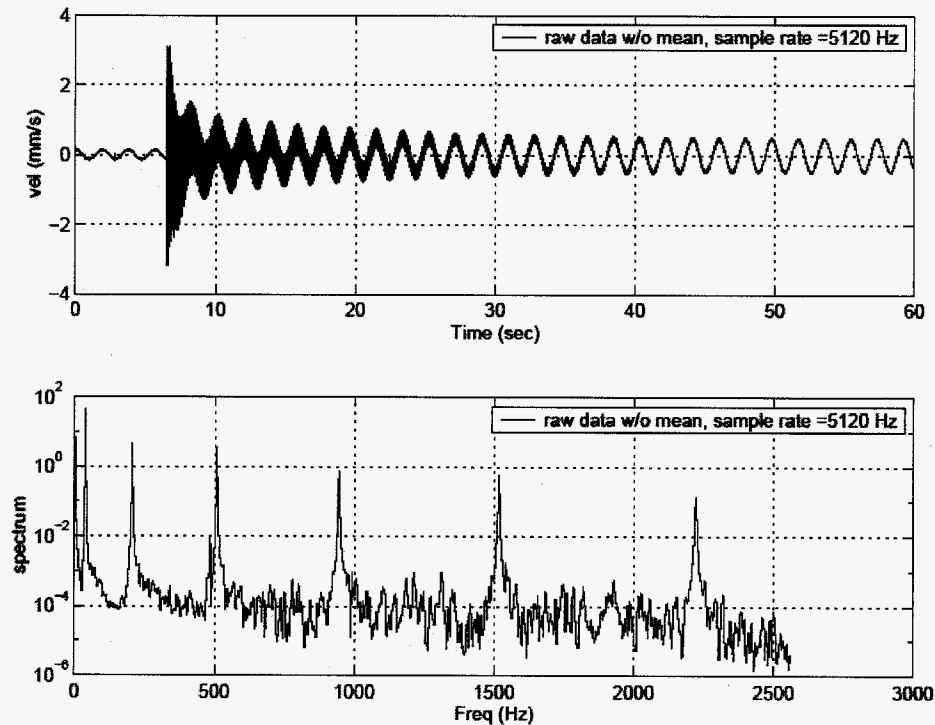


Figure 7. Typical Velocity Measurement of Specimen Vibration Decay

#### 4. THE ZENER DAMPING THEORY

The Zener theory relates damping  $\xi$  to temperature, material properties, thickness, and vibration frequency  $\omega$  as follows:

$$\xi = \frac{\alpha^2 ET}{2C_p \rho} \left[ \frac{\omega \tau}{1 + (\omega \tau)^2} \right]$$

$$\tau = \frac{C_p h^2 \rho}{\kappa \pi^2}$$

in which  $\alpha$  is coefficient of thermal expansion (1/K),  $h$  is specimen thickness (m),  $E$  is elastic modulus (N/m<sup>2</sup>),  $T$  is temperature (K),  $C_p$  is specific heat (J/kg/K),  $\kappa$  is thermal conductivity (W/m/K),  $\rho$  is density (kg/m<sup>3</sup>),  $\omega$  is frequency of vibration (rad/sec),  $\pi$  is 3.14159, and  $\tau$  is relaxation time (sec/rad). It is frequently more convenient to work with the relaxation frequency (1/ $\tau$ ) instead.

For b.c.c. and f.c.c. cubic lattice structured metals, Zener theory predicts the thermo-elastic energy loss in beams undergoing cyclic bending strains. Dependence on temperature, frequency, and beam thickness are captured in the theory; however, the theory does not apply for axial and torsional strains, for materials other than b.c.c. and f.c.c. metals, or for configurations other than rectangular beams. Many room temperature damping measurements have been made to validate the Zener theory, with much success [5, 6, 7, 8]. Predictive models for material damping in fiber-reinforced composites have been proposed and the available models have been summarized in detail [9].

Representative thermo-mechanical properties for Aluminum 6061-T6 were based on handbook values and are summarized in Table 1 [10, 11]. Note that  $\alpha$ ,  $C_p$ , and  $\kappa$  have a strong dependence on temperature. The coefficients of thermal expansion for Titanium 15-3-3-3 in Table 2 were obtained by interpolating the test data measured from 17 K to 300 K by COI [12]. The rest of properties for Titanium 15-3-3-3 were taken from [13, 14, 15] and are listed in Table 2.

During this damping study, samples of same material in various thickness were tested. The purpose is to investigate the change of damping as a function of frequency and correlate the results to the Zener damping theory, which predicts material damping as a function of temperature, modal frequency (or sample thickness), coefficient of thermal expansion and other thermal properties. If we can better understand which of these thermo-mechanical material properties influences the trends of damping at cryogenic temperatures then we can perhaps identify other materials appropriate for very stable cryogenic mechanical systems.

Table 1. Thermo-Mechanical Properties for Aluminum 6061-T6

	<u>T = 293 K</u>	<u>T = 40 K</u>
$\alpha$ (K <sup>-1</sup> ) [10]	22.86e-6	15.86e-06
E (N/m <sup>2</sup> ) [10]	68.948e9	73.602e9
$C_p$ (J/kg/K) [11]	897	77.5
$\rho$ (kg/m <sup>3</sup> ) [11]	2713	2713
$\kappa$ (W/m/K) [11]	158	88.5

Table 2. Thermo-Mechanical Properties for Titanium 15-3-3-3

	<u>T = 293 K</u>	<u>T = 40 K</u>
$\alpha$ (K <sup>-1</sup> ) [12]	8.87e-6	1.54e-06
E (N/m <sup>2</sup> ) [13]	1.05e11	1.10e11*
$C_p$ (J/kg/K) [14]	527.5	73.7
$\rho$ (kg/m <sup>3</sup> ) [13]	4761	4761
$\kappa$ (W/m/K) [15]	8.69	1.74

\* Scaled by the square of measured frequency ratio between 293 K and 40 K

## 5. RESULTS

All of the results described herein were measured using 2 inch wide and 20 inch long specimens of various thickness. Testing samples of various thickness provides damping values as a function of vibration frequency which is a driving parameter in the Zener damping equation. The tests were conducted in the Cryocooler Characterization Lab at the Jet Propulsion Laboratory, as described in Section 2.

### 5.1 Aluminum 6061-T6

Table 3 summarizes the measured damping values and fundamental frequencies at 293 K and 40 K of the three samples of aluminum 6061-T6. The first column in Table 6-1 shows the thickness (H), width (W) and length (L) of each sample. One of the original objectives of these tests was to check the test setup and procedures by repeating some of the tests reported previously [4].

Table 3. Measured Damping Values and Frequencies for Aluminum 6061-T6 at 293 K and 40 K

Specimen H x W x L (in)	$\zeta_{293}$ (%)	$\zeta_{40}$ (%)	Ratio $\zeta_{40} / \zeta_{293}$	$f_{293}$ (Hz)	$f_{40}$ (Hz)	Ratio $f_{40} / f_{293}$
1/12 x 2 x 20	0.084	0.0015	0.017	44.44	46.84	1.054
1/8 x 2 x 20	0.039	0.0017	0.044	63.59	66.99	1.053
1/4 x 2 x 20	0.0075	0.00055	0.073	125.64	132.38	1.054

Viscous damping values versus temperature are shown in Figure 8. Fundamental frequencies versus temperature are shown in Figure 9. It is observed from Table 3 and Figure 8 that the cryogenic damping at 40 K is decreased significantly to be as low as only 2% of the room-temperature damping at 293 K. The fundamental frequencies (or material stiffness properties) are increased slightly by about 5% from room temperature at 293 K to cryogenic temperature at 40 K, as shown in Table 3 and Figure 9.

Table 4. Measured Damping Compared to Zener Theory for Aluminum 6061-T6 at 293 K and 40 K

Specimen H x W x L (in)	$\zeta_{293, \text{measured}}$ (%)	$\zeta_{293, \text{Zener}}$ (%)	Ratio $f_{293, \text{measured}} / f_{293, \text{Zener}}$	$\zeta_{40, \text{measured}}$ (%)	$\zeta_{40, \text{Zener}}$ (%)	Ratio $f_{40, \text{measured}} / f_{40, \text{Zener}}$
1/12 x 2 x 20	0.084	0.088	1.95	0.0015	0.051	0.32
1/8 x 2 x 20	0.039	0.034	6.29	0.0017	0.088	1.02
1/4 x 2 x 20	0.0075	0.0044	49.7	0.00055	0.022	8.07

The viscous damping measurements at 293 K and 40 K have been compared to those predicted by the Zener theory in Table 4 of the three samples of aluminum 6061-T6 tested. The ratios of the free vibration frequency divided by the Zener relaxation frequency are also computed and listed in the table.

At the room temperature of 293 K, one can observe that the measured damping values and those predicted by the Zener theory agree reasonably well when the frequencies ratios are close to one. The close agreement serves to validate the experimental approach and data analysis techniques. The Zener theory underestimates damping at higher frequency ratios, a trend which has also been reported by other studies [4, 7, 8].

At the cryogenic temperature of 40 K, the damping measurements and the theory do not agree well for all frequency ratios. It is apparent that the Zener theory overestimates the damping at cryogenic temperatures for Aluminum 6061-T6.

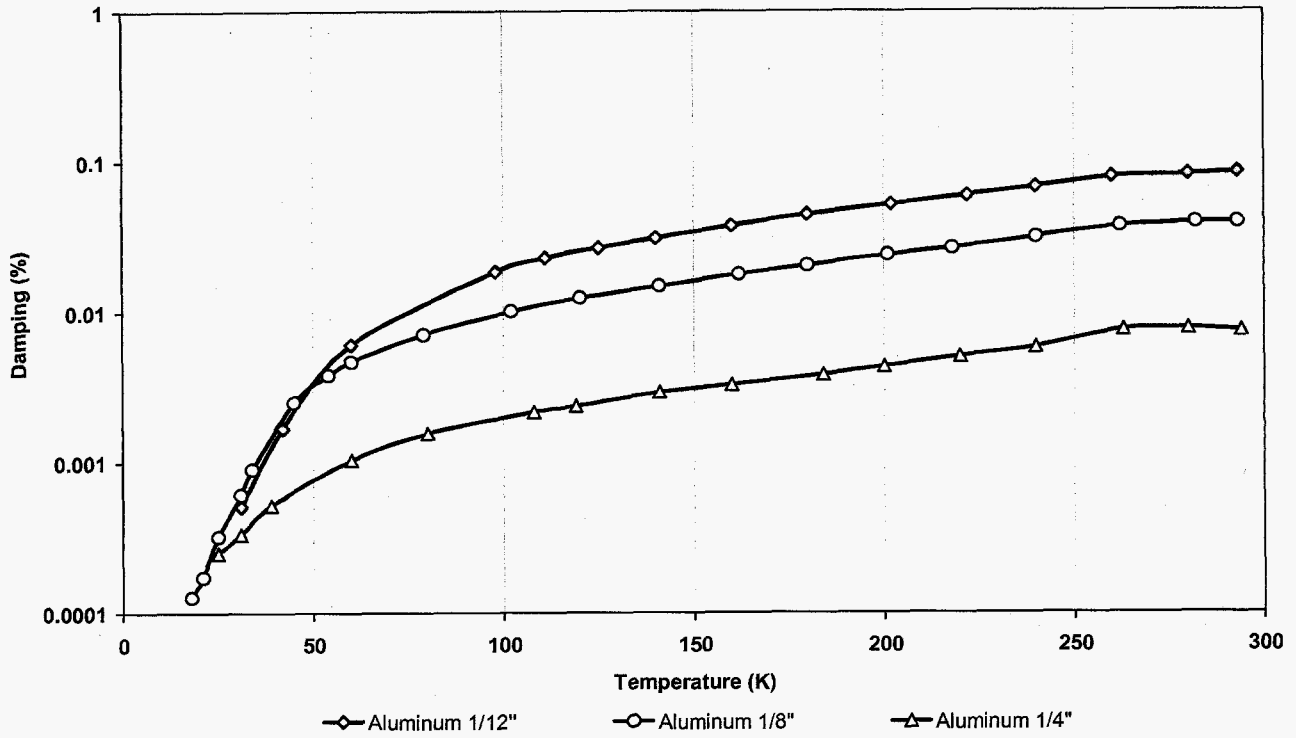


Figure 8. Measurements of Damping Values vs. Temperatures for Aluminum 6061-T6 Samples

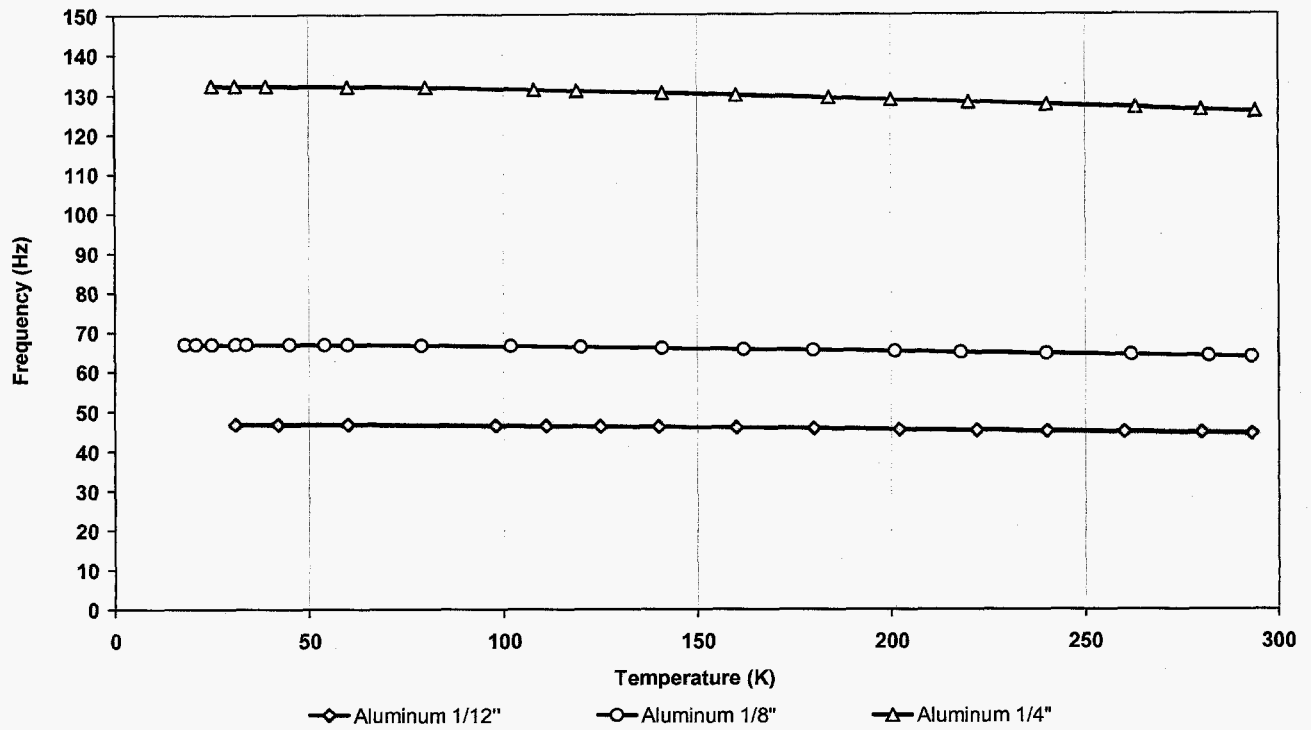


Figure 9. Measurements of Frequencies vs. Temperatures for Aluminum 6061-T6 Samples

## 5.2 Aluminum/Terbium/Dysprosium

TPF's ability to meet its ambitious science goals will be significantly enhanced by increasing its structural damping. The system's response to dynamic disturbances is proportional to  $1/2\zeta\omega_0^2$ . Given the low inherent damping of cryogenic materials, significant reduction in vibration amplitude could be gained with only modest increases in damping on the structure.

To examine the use of structural damping options to improve the dynamic stability of the cryogenic structure, an initial assessment was conducted experimentally on the use of magnetoelastic materials to achieve increased levels of cryogenic damping.

In magnetoelastic materials, the damping of vibrational energy occurs by a fundamentally different mechanism which is effective at low temperatures, for very small strains ( $< 10^{-1}\mu\epsilon$ ) and for very low frequencies ( $< 1$  Hz). Terbium (Tb) and dysprosium (Dy) are rare earth elements with large magnetic damping at cryogenic temperatures. A 30% energy loss per stress-strain cycle (in extension) in polycrystalline Tb/Dy has been measured at 77 K under quasi-static conditions.

To investigate the possibility of increasing the dynamic damping of bare aluminum under bending, both sides of an aluminum sample (1/8" x 2" x 20") were cleaned and coated by Tb/Dy through vapor deposit technique. The thickness of the coating is 1.6 microns or 16,000 Angstroms (1 Angstrom =  $1e-10$  meters =  $3e-9$  inches). Two sets of damping tests were conducted with the Tb/Dy coated aluminum sample and with the bare aluminum sample, respectively. The measured damping and frequency data at 293 K and 40 K, respectively, are compared with those of the bare aluminum sample in Table 5.

Viscous damping values versus temperature are compared with those of the bare aluminum sample in Figure 10. From the figure and Table 5, it is demonstrated no changes in damping at cryogenic temperatures ( $< 50$  K), while showing a measurable increase in damping as the temperatures higher than 50 K. At the room temperature of 293 K, the damping is increased by 15% from 0.039% to 0.045%, as shown in Table 5.

Fundamental frequencies versus temperature are compared with those of the bare aluminum sample in Figure 11. Both Terbium and Dysprosium are heavy elements. As a result of mass increase, the Tb/Dy coated aluminum sample shows a measurable decrease in frequency in both Figure 11 and Table 5. At the cryogenic temperature of 40 K, the fundamental frequency is decreased by about 0.6 %.

In summary, testing of a Tb/Dy coated Al sample under bending, through 1.6 micron vapor deposit technique, demonstrated no changes in cryogenic damping compared to the bare aluminum sample, while showing a measurable increase in mass. It is concluded that the vapor deposit of Tb/Dy is not an effective method to incorporate additional Tb/Dy damping into a TPF-like structural system. Presently at JPL, the maximum thickness can be achieved by the vapor deposit method is 5 microns or 50,000 Angstroms. More effective methods need to be investigated so that polycrystalline Tb/Dy can be incorporated into a structure for additional magnetoelastic damping at cryogenic temperatures.

Table 5. Measured Damping Values and Frequencies for Al/Tb/Dy vs. Aluminum 6061-T6

Aluminum H x W x L (in)	$\zeta_{293}$ (%)	$\zeta_{40}$ (%)	Ratio $\zeta_{40} / \zeta_{293}$	$f_{293}$ (Hz)	$f_{40}$ (Hz)	Ratio $f_{40} / f_{293}$
1/8 x 2 x 20	0.039	0.0017	0.044	63.59	66.99	1.053
Al/Tb/Dy H x W x L (in)	$\zeta_{293}$ (%)	$\zeta_{40}$ (%)	Ratio $\zeta_{40} / \zeta_{293}$	$f_{293}$ (Hz)	$f_{40}$ (Hz)	Ratio $f_{40} / f_{293}$
1/8 x 2 x 20	0.045	0.0017	0.038	63.30	66.60	1.052

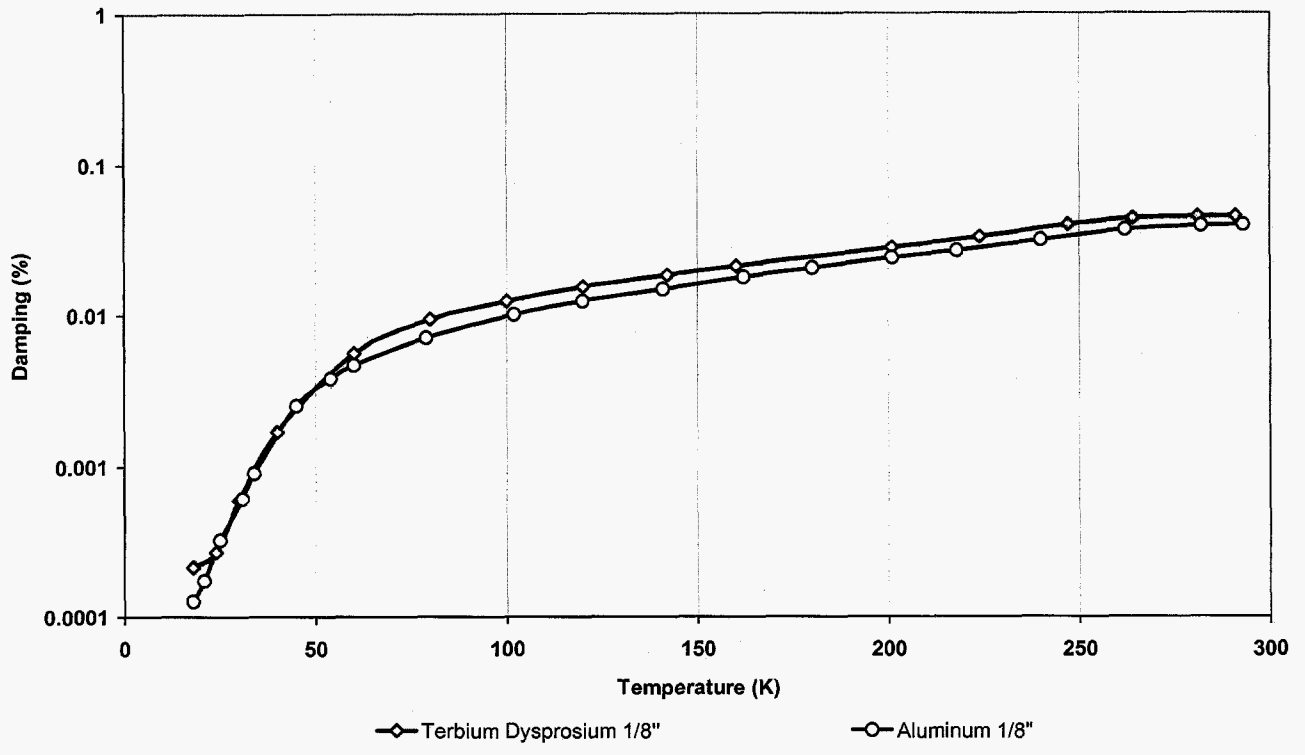


Figure 10. Measured Damping Values vs. Temperatures of Tb/Dy-Coated Aluminum and Bare Aluminum

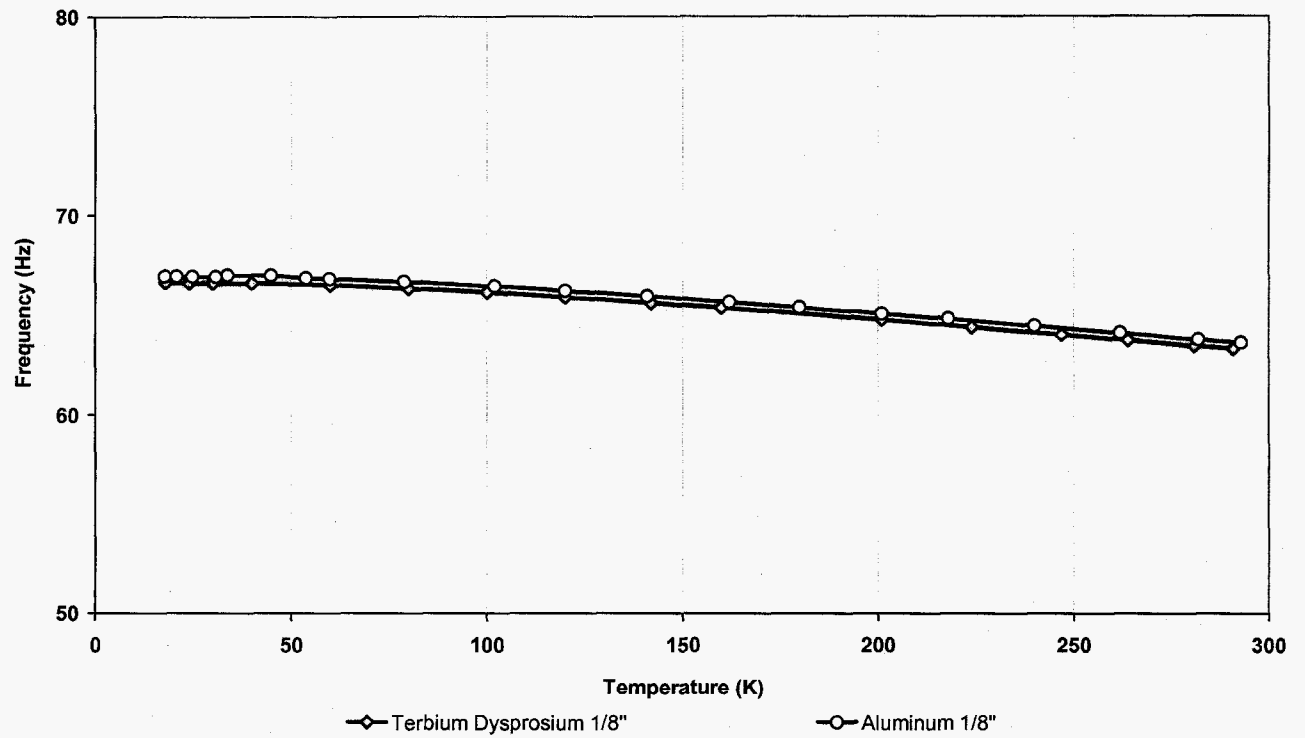


Figure 11. Measured Frequencies vs. Temperatures of Tb/Dy-Coated Aluminum and Bare Aluminum

### 5.3 Titanium

Titanium 15-3-3-3 was originally developed as a golf club technology for its desired damping properties at room temperature and is currently being used in cryocooler cold finger designs. This motivated us to test this material for detailed damping properties, especially at cryogenic temperatures. This section summarizes the fascinating test results that we have collected to date.

Titanium samples measuring 2 inch by 20 inch and of various thicknesses were tested. Table 6 summarizes the key dimensions. The damping ratios and fundamental frequencies measured on these samples are also shown, and compared at 293 K and 40 K, respectively, in Table 6. Viscous damping ratios versus temperature are shown in Figure 12. Fundamental frequencies versus temperature are shown in Figure 13.

Note that titanium 15-3-3-3 shows a remarkable increase in damping at cryogenic temperatures, as shown in Figure 12. The damping values at 40 K are 4 to 24 times higher than that at 293 K, as listed in Table 6. In contrast to the damping, the fundamental frequencies (or material stiffness properties), shown in Figure 13, are not sensitive to the temperature change from room temperatures to cryogenic temperatures. The frequencies are increased very slightly only by about 2.5% from 293 K to 40 K, as computed in Table 6.

In comparison to Table 3 and Figure 8 of aluminum samples, it is very exciting to observe that testing of Titanium 15-3-3-3 at cryogenic temperatures demonstrated over one order of magnitude increase in damping. As shown in Figure 12 and Table 6, damping of this material is about 0.1% at cryogenic temperatures, and given its other properties (e.g., good stiffness and low conductivity) this may become a viable candidate for applications on TPF-like structures.

Table 6. Measured Damping Values and Frequencies for Titanium 15-3-3-3 at 293 K and 40 K

Specimen H x W x L (in)	$\zeta_{293}$ (%)	$\zeta_{40}$ (%)	Ratio $\zeta_{40} / \zeta_{293}$	$f_{293}$ (Hz)	$f_{40}$ (Hz)	Ratio $f_{40} / f_{293}$
0.03 x 2 x 20	0.017	0.070	4.12	14.13	14.43	1.022
0.04 x 2 x 20	0.011	0.050	4.55	17.64	18.09	1.026
0.06 x 2 x 20	0.0042	0.054	12.86	27.41	28.12	1.026
0.09 x 2 x 20	0.0029	0.071	24.48	37.27	38.14	1.024

In Table 7, the damping values predicted by the Zener damping model are compared to both room temperature and cryogenic temperature measurements of Titanium 15-3-3-3 on the four different sample thicknesses. The corresponding ratios of the free vibration frequency divided by the Zener relaxation frequency are also tabulated in Table 7.

At the room temperature of 293 K, the measured damping values are predicted very well by the Zener theory, especially as the frequencies ratios are close to one. This validates the experimental approach and data analysis techniques. As for the aluminum samples, the Zener theory underestimates damping at higher frequency ratios. However, at the cryogenic temperature of 40 K, the damping measurements can not be predicted by the theory at all for all frequency ratios. The theory underestimates the damping by more than one order of magnitude.

Table 7. Measured Damping Compared to Zener Theory for Titanium 15-3-3-3 at 293 K and 40 K

Specimen H x W x L (in)	$\zeta_{293, \text{measured}}$ (%)	$\zeta_{293, \text{Zener}}$ (%)	Ratio $f_{293, \text{measured}} / f_{293, \text{Zener}}$	$\zeta_{40, \text{measured}}$ (%)	$\zeta_{40, \text{Zener}}$ (%)	Ratio $f_{40, \text{measured}} / f_{40, \text{Zener}}$
0.03 x 2 x 20	0.017	0.022	1.51	0.070	7.36e-4	1.07
0.04 x 2 x 20	0.011	0.013	3.35	0.050	5.24e-4	2.40
0.06 x 2 x 20	0.0042	0.0041	11.7	0.054	1.73e-4	8.38
0.09 x 2 x 20	0.0029	0.0013	35.8	0.071	5.76e-5	25.6

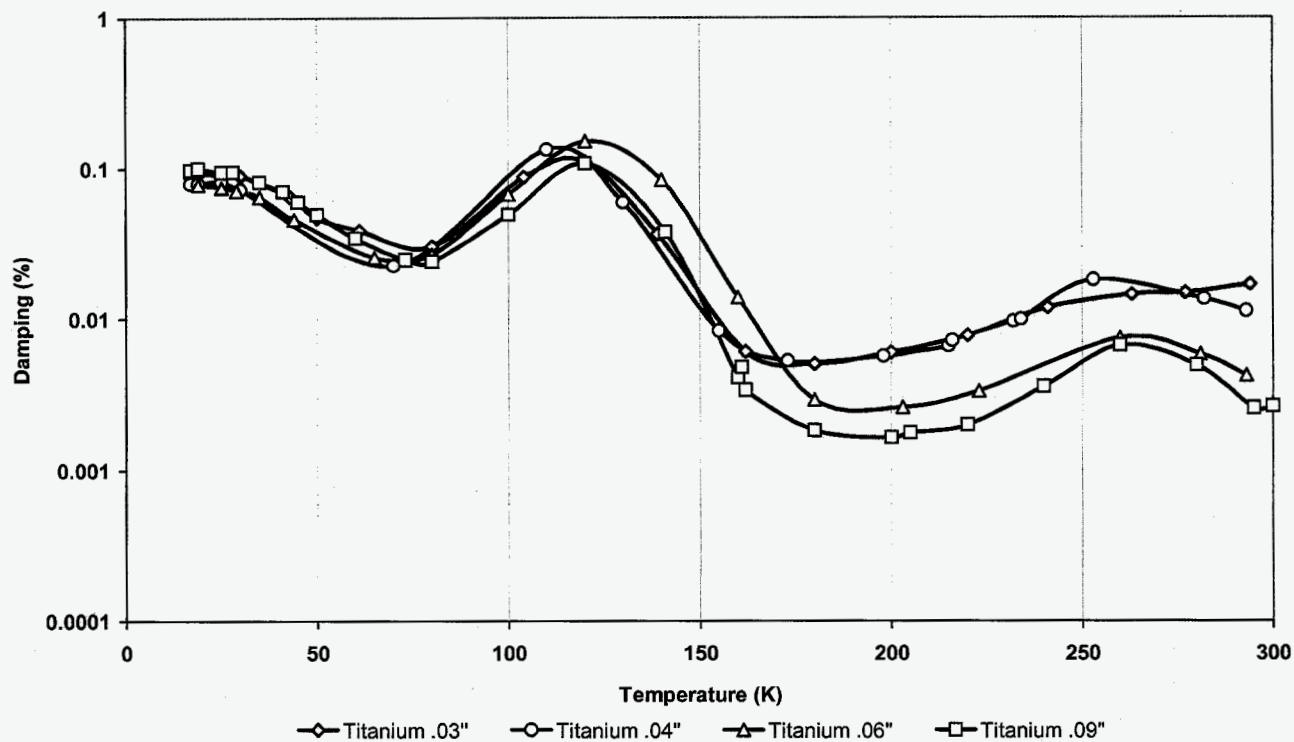


Figure 12. Measurements of Damping Values vs. Temperatures for Titanium 15-3-3-3 Samples

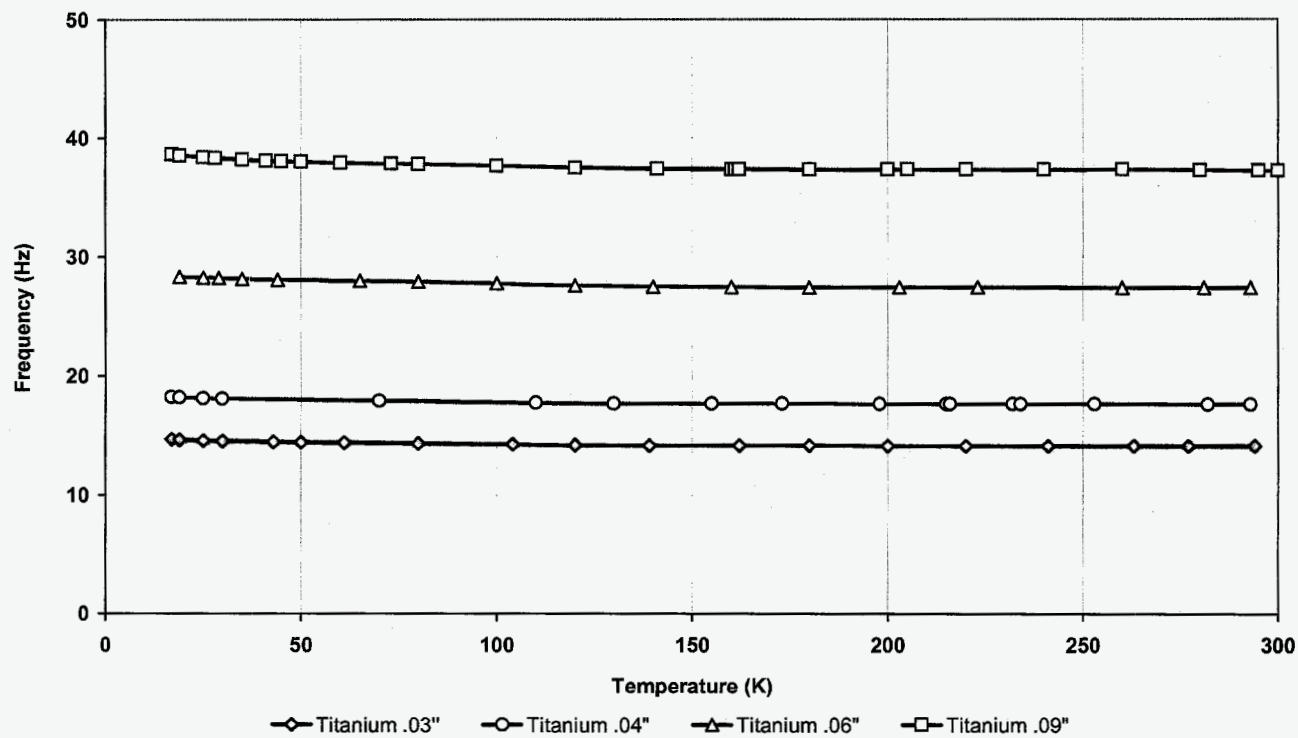


Figure 13. Measurements of Frequencies vs. Temperatures for Titanium 15-3-3-3 Samples

## 5.4 Composites

To support the TPF Structurally Connected Interferometer (SCI) study, both Lockheed Martin Aerospace (LMA) and Ball Aerospace Systems (BAS) provided graphite composite laminate samples for cryogenic damping evaluation at JPL. The fiber types and key dimensions of LMA and BAS samples are listed in the first column of Table 8 and Table 9, respectively. The damping ratios and fundamental frequencies measured on these samples at 293 K and 40 K are also summarized in the tables.

Damping values measured on LMA and BAS samples are presented graphically in Figure 14 and Figure 16, respectively. The present damping measurements at both room and cryogenic temperatures compare closely with those reported previously. As shown by the damping vs. temperature plots in Figures 14 and 16 and the damping ratios in Tables 8 and 9, the graphite composite samples tested during the present study follow the general trend of decreasing damping with decreasing temperature. However, it is observed that the damping reduction of the graphite composite samples from room to cryogenic temperatures is less significant than that of the aluminum samples. The ratios of  $\zeta_{40}/\zeta_{293}$  are between 22% and 50% for the graphite composite samples that are much higher than the ratios for the aluminum samples.

Fundamental frequencies measured on LMA and BAS samples are presented graphically in Figure 15 and Figure 17, respectively. From the figures and the frequency ratios listed in Tables 8 and 9, it is evident that frequencies (or stiffness properties) of the graphite composite samples are much less sensitive to temperatures than those of aluminum samples.

Table 8. Measured Damping Values and Frequencies for Composites at 293 K and 40 K (LMA)

<b>K13C2U</b> <b>H x W x L (in)</b>	$\zeta_{293}$ (%)	$\zeta_{40}$ (%)	<b>Ratio</b> $\zeta_{40}/\zeta_{293}$	$f_{293}$ (Hz)	$f_{40}$ (Hz)	<b>Ratio</b> $f_{40}/f_{293}$
1/16 x 2 x 20	0.0146	0.00417	0.2856	71.70	71.54	0.9978
1/8 x 2 x 20	0.0154	0.00440	0.2857	136.29	135.93	0.9974
3/16 x 2 x 20	0.0166	0.00518	0.3120	202.61	202.29	0.9984
<b>M55J(6K)</b> <b>H x W x L (in)</b>	$\zeta_{293}$ (%)	$\zeta_{40}$ (%)	<b>Ratio</b> $\zeta_{40}/\zeta_{293}$	$f_{293}$ (Hz)	$f_{40}$ (Hz)	<b>Ratio</b> $f_{40}/f_{293}$
1/16 x 2 x 20	0.02126	0.01072	0.5042	55.94	55.39	0.9901
1/8 x 2 x 20	0.02286	0.01070	0.4681	106.88	105.98	0.9915
3/16 x 2 x 20	0.02369	0.01046	0.4415	158.03	156.71	0.9916

Table 9. Measured Damping Values and Frequencies for Composites at 293 K and 40 K (BAS)

<b>K13C2U</b> <b>H x W x L (in)</b>	$\zeta_{293}$ (%)	$\zeta_{40}$ (%)	<b>Ratio</b> $\zeta_{40}/\zeta_{293}$	$f_{293}$ (Hz)	$f_{40}$ (Hz)	<b>Ratio</b> $f_{40}/f_{293}$
0.0365 x 2 x 20	0.01403	0.003940	0.2808	43.28	43.24	0.9991
0.0725 x 2 x 20	0.01886	0.004146	0.2198	79.20	79.14	0.9992
0.11 x 2 x 20	0.01603	0.004738	0.2956	117.74	117.62	0.9990

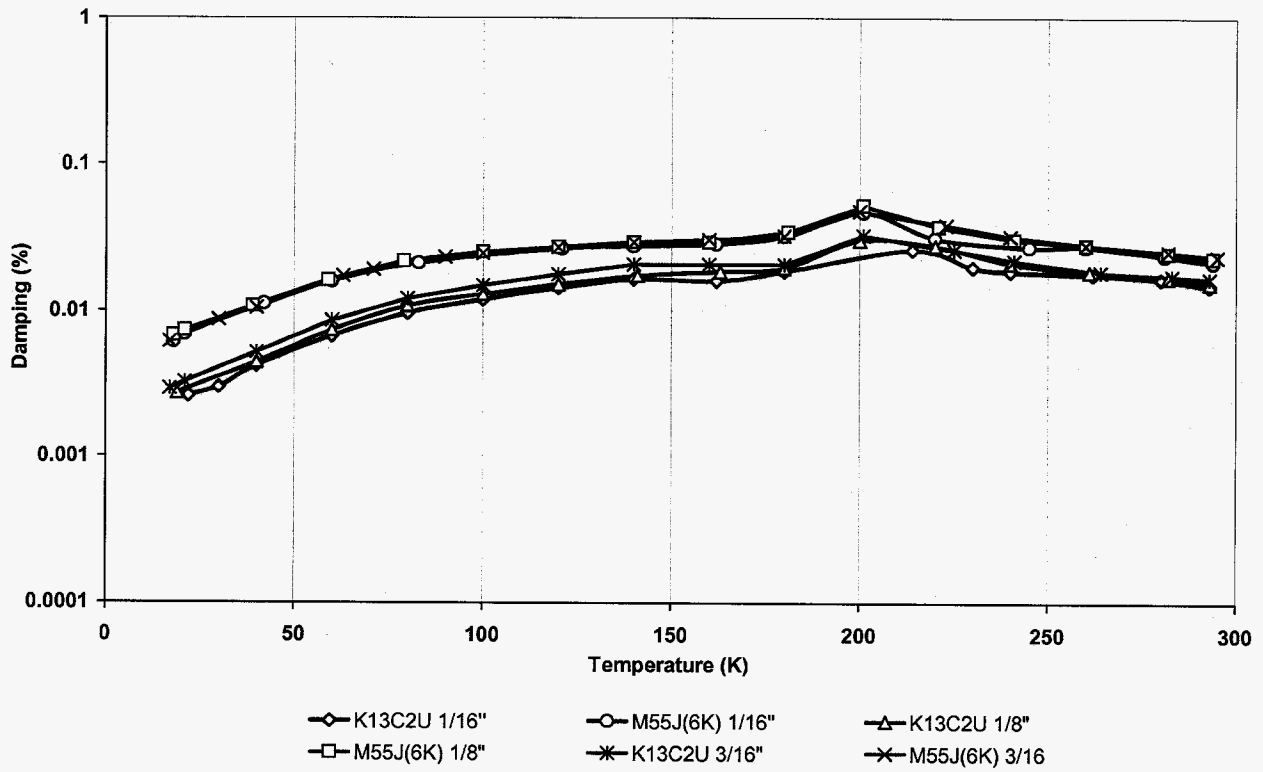


Figure 14. Measurements of Damping Values vs. Temperatures for Composite Samples (LMA)

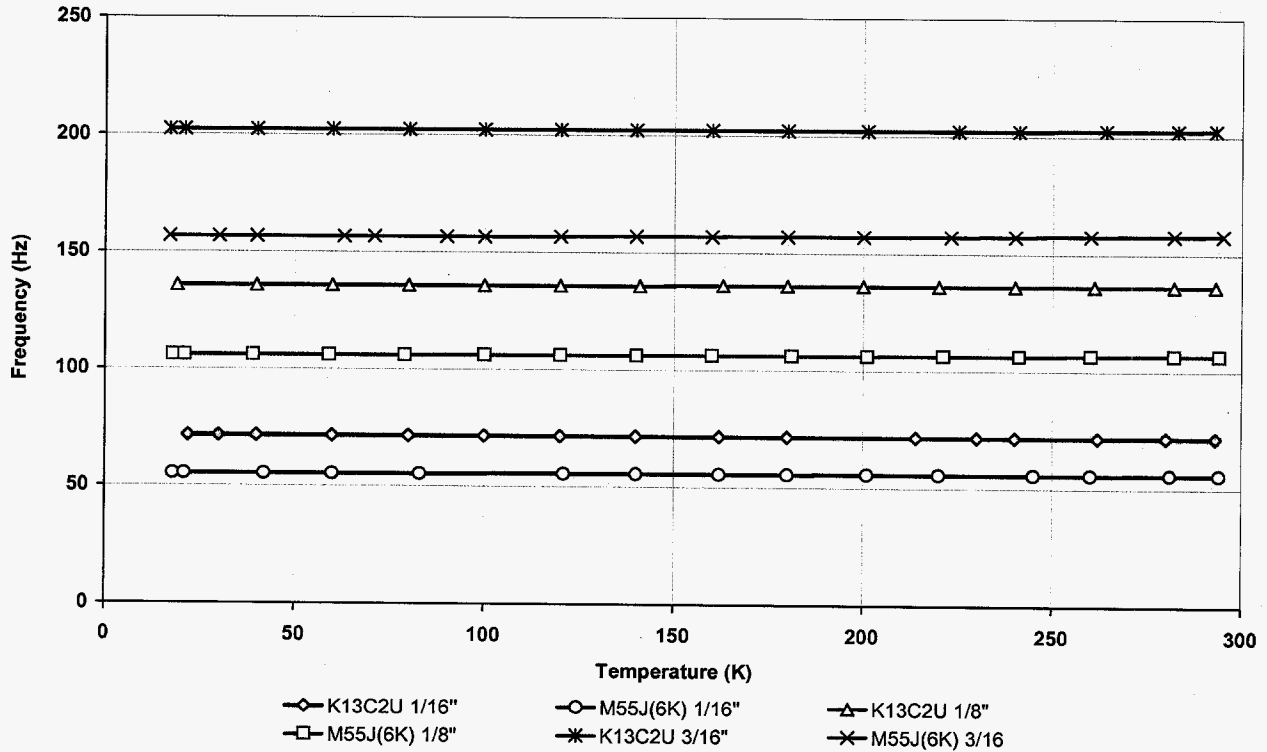


Figure 15. Measurements of Frequencies vs. Temperatures for Composite Samples (LMA)

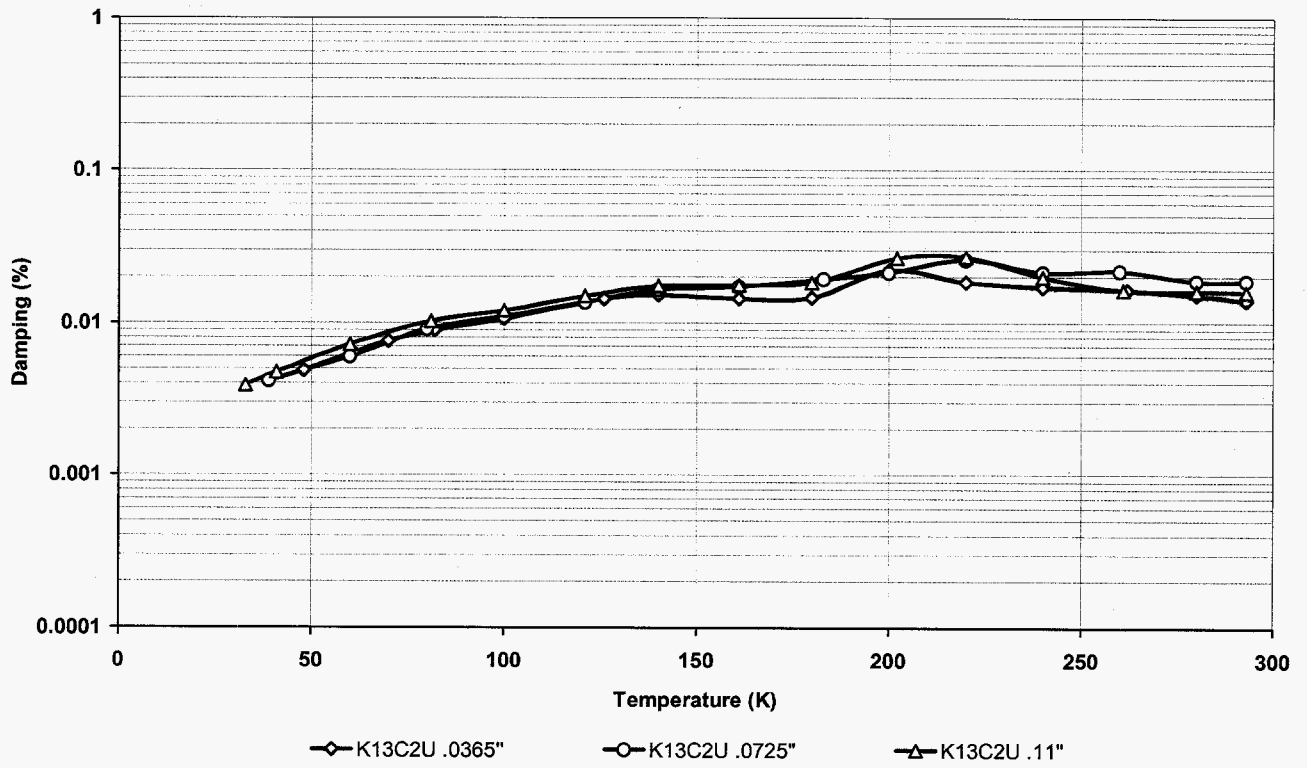


Figure 16. Measurements of Damping Values vs. Temperatures for Composite Samples (BAS)

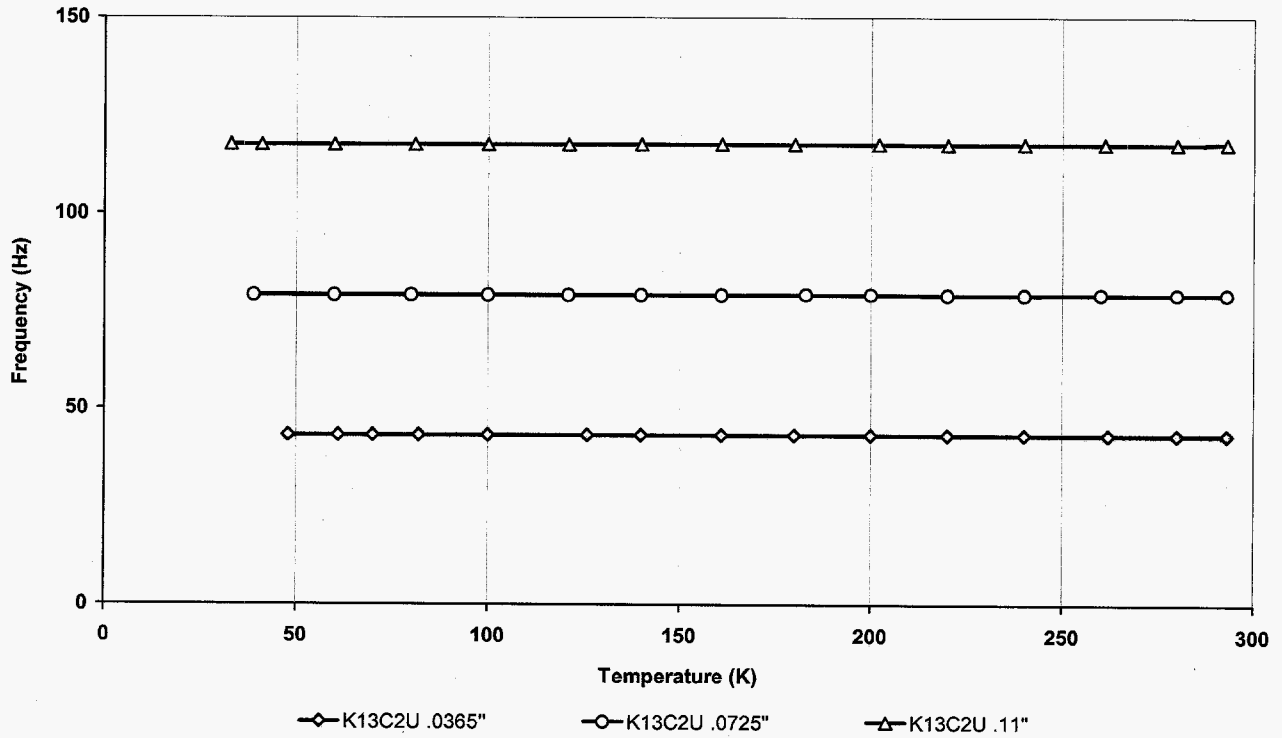


Figure 17. Measurements of Frequencies vs. Temperatures for Composite Samples (BAS)

## 6. CONCLUSIONS

To meet the challenging requirements of the TPF mission, an intensive experimental effort has been conducted to provide an insight into the material damping levels at cryogenic temperatures and to search for materials with high cryogenic damping. The test results will enable accurate system level models for prediction and control of instrument disturbances and will improve the dynamic stability of cryogenic structures for TPF. All material damping measurements were performed with a unique test setup in the Cryocooler Characterization Lab at the Jet Propulsion Laboratory.

Supported by the measurements described in this paper, the following summarizes key observations on the material damping at cryogenic temperatures:

- Except for Titanium 15-3-3-3, the test data shows the general trend of decreasing damping with decreasing temperature, but the amount of the damping decrease is a function of frequency and material.
- Aluminum 6061-T6 shows a significant monotonic decrease in viscous damping at cryogenic temperatures. The damping of Aluminum 6061-T6 at cryogenic temperature 40 K can be as low as only 2% of the damping at room temperature 293 K. The cryogenic damping can be decreased to the order of  $10^{-4}$  % below 40 K.
- It is concluded that the vapor deposit of Tb/Dy is not an effective method to incorporate additional magnetoelastic damping into a TPF-like structural system at cryogenic temperatures. Testing of a Tb/Dy coated Aluminum 6061-T6 sample under bending, through 1.6 micron vapor deposit technique, demonstrated almost no increase in cryogenic damping compared to the bare aluminum sample, while showing a measurable penalty in mass.
- Titanium 15-3-3-3 shows a remarkable increase in damping at cryogenic temperatures. It demonstrates over one order of magnitude increase in damping in comparison to aluminum. Given its other properties (e.g., good stiffness and low conductivity) this may prove itself to be a good candidate for the application on TPF-like structures.
- The graphite composite samples tested during the present study follow the general trend of decreasing damping with decreasing temperature. However, the damping reduction from room to cryogenic temperatures is less significant than that of the aluminum samples. The ratios of  $\zeta_{40}/\zeta_{293}$  are between 22% and 50% that are much higher than aluminum.
- The applicability of the Zener damping theory is confirmed for aluminum and titanium at room temperatures. However, large discrepancies at cryogenic temperatures between the Zener theory and the test data are observed.

Note that these material damping measurements and the observations described above are valid for rectangular beams subjected to bending strains only. Different damping values may be measured as a function not only of material, temperature and frequency, but also of geometry, configuration, strain sense, strain amplitude and environmental effects.

## ACKNOWLEDGEMENT

The authors would like to thank Steve Gunter for his coordination between the Cryogenic Structures Technology task and other TPF Interferometer Technology Demonstration & Testbed tasks.

The management support by Curt Henry from the TPF Interferometer Systems team is gratefully acknowledged.

The authors also would also like to thank Lee Peterson/Jason Hinkle from the University of Colorado at Boulder, Doug Adams from Jet Propulsion Laboratory and Bob Coppolino from Measurement Analysis Corporation for their technical inputs and discussions.

It is greatly appreciated that Ron Ross introduced the material of Titanium 15-3-3-3; Paul Van Velzer and Jennifer Dooley helped to coat aluminum samples with Tb/Dy at JPL; COI Testing Service provided timely measurements of Titanium's coefficient of thermal expansion; and Lockheed Martin Aerospace and Ball Aerospace Systems agreed to publish the material damping data tested by JPL for them during the TPF Structurally Connected Interferometer study.

This work was performed at the Jet Propulsion Laboratory, California Institute of Technology, under contract with the National Aeronautics and Space Administration.

## REFERENCES

1. G. W. Bush, "*A Renewed Spirit of Discovery: the President's Vision for U.S. Space Exploration*," U.S. White House Document, January 2004.
2. Curt Henry, Oliver Lay, MiMi Aung, Steven Gunter, Serge Dubovitsky, Gary Blackwood, "*Terrestrial Planet Finder Interferometer: architecture, mission design and technology development*," SPIE Astronomical Telescopes and Instrumentation, Glasgow, Scotland, June 22, 2004.
3. Marie Levine, Gregory Moore, Scott A. Basinger, Andrew Kissil, Eric Bloemhof, Steve Gunter, "*Integrated Modeling Approach for the Terrestrial Planet Finder Mission*," SPIE Astronomical Telescopes and Instrumentation, Glasgow, Scotland, June 22, 2004.
4. M. B. Levine and C. V. White, "*Experiments to Measure material Damping at Cold Temperatures*," JPL-JWST-FTM-0010/D-22047, Jet Propulsion Laboratory, Pasadena, CA 91109, September 29, 2002.
5. Ting, J., E.F. Crawley, "*Characterization of Damping of Materials and Structures at Nanostrain Levels*," M.S. Thesis, M.I.T., June 1990.
6. Crawley, E.F., G. L. Sarver, and D.G. Moore, "*Experimental Measurement of Passive Material and Structural Damping for Flexible Space Structures*," Acta Astronautica, Vol. 10, No. 5-6, 1983.
7. Crawley, E.F., M.C. Van Schoor, "*Material Damping in Aluminum and Metal Matrix Composites*," Journal of Composite Materials, Vol. 21, Jun. 1987.
8. Crawley, E.F., R.L. Sheen, "*Experimental Measurement of Material Damping for Space Structures*," Proc. Of Vibration Damping Workshop, Long Beach, CA, Feb. 1983.
9. Chandra, R., S. P. Singh, K. Gupta, "*Damping Studies in Fiber-Reinforced Composites – A Review*," Composite Structures, Vol. 46, 1999.
10. Cryogenic Materials Data Handbook, Air Force Materials Laboratory-Research and Technology Division, Wright-Patterson AFB, July 1965.
11. Cryocomp Computer Program, Version 3.05, Eckels Engineering, Inc., Florence, SC.
12. Steve Connell, Test Data of Titanium's Coefficient of Thermal Expansion (Excel format), COI Testing Service, June 10, 2004.
13. MIL-HDBK-5H, , Pg. 5-130, Table 5.5.2.0(b) - Design Mechanical and Physical Properties of Ti-15V-3Cr-3Sn-3Al Sheet, Figure 5.5.2.0 - Effect of temperature on the physical properties of Ti-15V-3Cr-3Sn-3Al alloy, December 1, 1998.
14. Thermophysical Properties of Matter, Vol. 4, Specific Heat, pp. 607-609, Curve 2 - Series 3 Data for Ti + V + SXi Alloys.
15. Thermophysical Properties of Matter, Vol. 1, Thermal Conductivity, pp1086-1088, Curve 2 & 5 Data for Ti + V + SXi Alloys.